NOTES AND CORRESPONDENCE

Radar Reflectivity–Ice Water Content Relationships for Use above the Melting Level in Hurricanes

ROBERT A. BLACK

NOAA/AOML, Hurricane Research Division, Miami, Florida

14 August 1989 and 6 February 1990

ABSTRACT

Regression equations linking radar reflectivity (Z_e) and ice water content (IWC) were calculated from airborne radar and particle image data that were collected above the melting level in two hurricanes. The Z_e–IWC equation from the stratiform areas of Hurricane Norbert (1984) is similar to the composite equation for thunderstorm anvils derived by Heymsfield and Palmer. The Z_e–IWC equation from the convective regions of Hurricane Irene (1981) has essentially the same exponent, but a significantly greater coefficient than that from Norbert. The higher density of the graupel and rounded ice in the Irene data accounts for the difference in the coefficients. The hurricane Z_e–IWC relations have smaller exponents than most of those from midlatitude clouds, which indicates that small ice particles may be more prevalent in these two hurricanes than in midlatitude clouds.

1. Introduction

The relationship between condensation heating and the wind field in hurricanes is not well understood. One method of diagnosing the heating is the determination of a water budget, which requires aircraft measurements of winds, cloud (suspended) water contents, and precipitation water contents through the storm volume. Marks and Houze (1987) developed techniques to estimate the wind field from airborne Doppler radar measurements. Cloud and precipitation water content can be readily estimated from the reflectivity data when the temperature (T) is >0°C. The estimation of cloud and precipitation water content at $T < 0$°C when ice particles are present is more difficult because of the variable shapes and densities of ice particles. The purpose of this study is the calculation of regression equations between equivalent radar reflectivity (Z_e) (Smith 1984) and ice water content (IWC) from in situ measurements obtained above the melting level in hurricanes.

The IWC can be estimated independently of Z_e either by direct capture or by particle imaging. With the direct capture method, ice particles are captured and melted. The IWC is derived from the diameters of the droplets that are left by the melted ice particles. In the second method, particle image data are used with empirical particle diameter-mass relations to estimate IWC if the particle shapes are known. Otherwise, the IWC is estimated assuming a particle shape and density.

Heymsfield and Palmer (1986) computed Z–IWC relations for Montana thunderstorm anvils from ground-based radar and airborne particle image data. Heymsfield (1977) and Herzegh and Hobbs (1980) used similar data to compute other equations that are valid for midlatitude frontal clouds. Sekhon and Srivastava (1970) and Gunn and Marshall (1958) calculated Z–rain rate (R), R–IWC, and Z–IWC regression equations. Their data were derived from ground-based radar data and IWCs that were estimated from ice particles captured and melted at the surface during snowstorms. These Z–IWC equations have been corrected for the smaller reflectivity of ice particles (Smith 1984) and are listed in Table 1.

Variations in Z–IWC relations reflect differences in the distribution of ice mass with particle size. The variability in the Z–IWC relations is illustrated by the fact that the fits tabulated in Table 1 give an IWC range from 0.4 to 2.7 g m^{-3} for Z_e = 30 dBZ.

Precipitating ice particles at the −5°C level in hurricanes have diameters from 0.1–5 mm (Black and Hallett 1986) and usually contain most of the condensate mass. The radar cross section of dry-surfaced ice particles in this size range is described by Rayleigh scattering and is principally a function of particle mass, not shape (Battan 1973; Smith 1984). This property makes it possible to develop Z–IWC relations. However, since the correlations between ice particle diameter, mass, and radar reflectivity factor are not linear, many different Z–IWC relations corresponding to other particle types and size distributions can be derived for a given total particle mass.

Corresponding author address: Robert A. Black, NOAA/AOML, Hurricane Research Division, 4301 Rickenbacker Causeway, Miami, FL 33149.

TABLE 1. Midlatitude z–IWC relations. All but the Gunn and Marshall (1958) equation were obtained from Heymsfield and Palmer (1986).

	Notes	References
$Z = 299*(IWC)^{1.48}$	Continental thunderstorm anvils	HP[a]
$Z = 575*(IWC)^{1.65}$	Warm frontal clouds	HH[b]
$Z = 151*(IWC)^{1.98}$	Deep cirriform clouds	H[c]
$Z = 12\,589*(IWC)^{2.57}$	Winter snowstorms, at the surface	SS[d]
$Z = 8318*(IWC)^{2.22}$	Winter snowstorms, at the surface	GM[e]

[a] Heymsfield and Palmer (1986) composite, Plank (1980) method.
[b] Herzegh and Hobbs (1980).
[c] Heymsfield (1977).
[d] Sekhon and Srivastava (1970).
[e] Gunn and Marshall (1958).

Hurricane Z–IWC relations may be different from those found in midlatitudes. Hurricane updrafts are usually weaker than continental thunderstorm updrafts (Jorgensen et al. 1985) and often contain higher concentrations of small diameter (<0.5 mm) ice and graupel than winter frontal clouds. Hurricane updrafts usually have much lower precipitation water contents above the melting level than continental thunderstorms (Black and Hallett 1986). In hurricanes, the most frequently observed ice particle types are irregular aggregates (stratiform areas) and graupel (convective areas). Columns and needles are the most commonly observed pristine crystal habits (Black and Hallett 1986), but they are relatively rare. These types of particles and the low water contents may cause much different ice particle mass distributions in hurricanes than are found in continental thunderstorms.

In this study, results from two methods of computing Z–IWC relations are presented: a two-pass method that also produces an effective ice particle bulk density and the method used by Heymsfield and Palmer (1986). The hurricane Z–IWC equations computed here are compared with those from midlatitude studies.

2. Data analysis procedures

This study is the first of its type to use simultaneous image and radar reflectivity data obtained in hurricanes. Particle images were acquired with the Particle Measuring Systems, Inc. (PMS) two-dimensional (2-D) optical array probes (Knollenberg 1981). Digitized radar reflectivity data were provided by the tail radar of the NOAA WP-3D aircraft. The 2-D probes measure particle cross-sectional shape and area as well as number concentration. The tail radar has a 3.2 cm wavelength, a horizontal beam width of 1.35°, and a vertical beam width of 1.9°. The radar completes a rotation in the plane perpendicular to the flight track in ~7.5 s. In this time, the aircraft flies ~1100 m at typical ground speeds.

Most of the data that were collected on 24 September 1984 in eastern Pacific Hurricane Norbert were obtained in stratiform areas outside the eyewall. On this day, the flight pattern was a series of rotating wedges, at the 6 km level, that were centered on the eye. Temperatures ranged from −4° to −8°C. The radial legs were ~30–110 km long and ~90° apart. Norbert was gradually weakening as it moved north, and there was little strong convection anywhere in the storm. The PMS probe images showed that the Norbert ice particles were irregularly shaped snow and columns. Measured flight-level equivalent reflectivities varied from 1–34 dBZ.

Data from within and near vigorous convection were obtained in Atlantic Hurricane Irene on 26 September 1981. In Irene, the flight pattern was designed to repeatedly fly downwind about the storm within the strongest convective rainband to maximize the amount of time spent in, and downwind from, the strongest convection. These particles were predominantly rounded ice and graupel (Black and Hallett 1986). At the ~6 km flight-level, radar reflectivities from the tail radar varied from 1–44 dBZ at temperatures from −3° to −6°C. The melting level was near 4.5 km. These storms represent the extreme cases from the standpoint of convective or stratiform data. No vigorous convection was sampled in Norbert, and little stratiform precipitation was observed in Irene. Henceforth, "stratiform" refers to the Norbert data, and "convective" means data from Irene.

Only data from the PMS 2D-P (0.2 mm ≤ diameter ≤ 6.4 mm) probe were used in this study. Water contents in the 0.05–0.2 mm size channels from the PMS 2D-C probe were rarely >5% of the 2D-P IWC and always contributed <1% of the reflectivity calculated from the 2D-P particle size distribution. The particle image data were analyzed and sized using the techniques described by Black and Hallett (1986). Those procedures reject all images whose longest dimension is on the edge of the image field and could conceivably bias the image data against large particles. Heymsfield and Palmer (1986) described the effects of truncation of the particle size spectra at a given maximum size on IWC_c and dBZ_c. The unprocessed 2D-P image data were inspected visually for evidence of very large (>6.4 mm) particles. No particles > 3 mm were observed in Norbert and very few particles > 5 mm diameter were observed in Irene. Therefore, no corrections were made for truncating the large end of the size spectra at 6.4 mm. All particle-size data were averaged for 10 s (~1.4 km) to insure representative spectra in areas with few particles.

The computed ice water content (IWC_c) from the particle image data was

$$IWC_c = \frac{\pi}{6} \rho \sum N_i D_i^3, \quad (1)$$

where ρ is the effective ice particle bulk density, N_i is

the number of images of size i per unit volume, and D_i is the diameter of the equivalent-area circle. Calculated equivalent radar reflectivity Z_c was obtained from the particle-size spectra assuming melted diameters:

$$Z_c = (P^2 * 0.224) \sum N_i D_i^6, \quad (2)$$

where P^2 is the (unitless) square of the numerical value of the effective ice particle bulk density. Smith (1984) showed that the factor 0.224 accounts for the smaller index of refraction of ice for microwave radiation.

Vertical radar reflectivity cross sections along the aircraft track were constructed by mapping the radar data from the near-vertical radials into 1000 m horizontal by 300 m vertical resolution bins. Radar data that fell within a bin was assumed to fill the entire bin. If more than one Z_e value was available in a bin, the Z_e values were averaged. Because the first acceptable data were 361 m from the aircraft, the mapping process left a 600 m void in the cross section centered on the aircraft position. Flight-level "measured" reflectivity (Z_m) was estimated by filling the bins in this void through linear interpolation of Z_e from the bins above and below the aircraft position. Thus, Z_m was in error to the extent that the vertical reflectivity gradient near the aircraft was not linear in Z_e. The interpolated reflectivity was most likely to be inaccurate in convective regions with strong vertical reflectivity gradients. However, unlike the estimates of flight-level reflectivity obtained from ground-based radar in most earlier studies, the procedure for determining Z_m in this research is free of attenuation, nonhomogeneous beam filling, and aircraft position errors.

The flight-level reflectivity values obtained by this method were occasionally checked against the horizontal average that was constructed using the procedure described above, but with the reflectivity values from the radials to the left and right of the aircraft heading. In general, there was close agreement between the horizontal and vertical versions of the flight-level radar reflectivity algorithm. The mean reflectivity difference (vertical − horizontal) was +1 dBZ, with a maximum difference of +7 dBZ for one sample. This bias results from a decrease in Z with height and is about equal to the intrinsic 0.85 dBZ standard deviation of the tail radar's reflectivity estimate (F. D. Marks, Jr., personal communication, 1989). The values of Z_m were not adjusted for this bias because it was similar in magnitude to the error of the measurement.

The PMS data were analyzed sequentially by time in blocks containing about 30 min of data. Each block was stored as a separate file on the computer. A two-pass algorithm was used on each file. On this first pass, Z_c and IWC_c were estimated assuming that all images were ice with an ice particle bulk density of 0.2 g cm^{-3} in Norbert and 0.7 g cm^{-3} in Irene. Then, the Z_m corresponding to each 10 s average particle-size spectrum was added to the file. The 10 s particle-size spectra were sorted by Z_m in 5 dBZ intervals for the range $1 < \mathrm{dBZ}_m \leq 50$.

The calculation of Z_c and IWC_c for the second pass requires an estimate of the ice particle bulk density ρ_e that is consistent with Z_m. Let ρ_1 be the initial guess for ρ_e from pass 1. The calculated reflectivity Z_c for each 10 s average particle size spectrum in a given reflectivity range is obtained from Eq. (2), and these estimates of Z_c are averaged. This mean reflectivity Z_{cm} is used to solve Eq. (2) for $\sum N_i D_i^6$:

$$\sum N_i D_i^6 = Z_{cm}(\rho_1 * 0.224)^{-1}. \quad (3)$$

Define Z_{mm} as the mean of the measured flight-level reflectivities from the tail radar cross section for the reflectivity range. Substituting this quantity and (3) into Eq. (2), the mean ice particle bulk density for the reflectivity category is easily computed:

$$\rho_e{}^2 = Z_{mm}(0.224 * \sum N_i D_i^6)^{-1}. \quad (4)$$

This procedure was used only when both 2D-P and tail radar reflectivity data were available. On the second pass, IWC_c and Z_c were recomputed for each file using the value of ρ_e from (4) for the value of Z_m that corresponded to the given 10 s average particle-size spectrum. Those periods for which ρ_e was >0.8 g cm^{-3} were deleted to exclude regions containing substantial amounts of liquid water. No regions with substantial liquid water existed in the Norbert data, but 2.2% of the Irene spectra from the first pass were excluded from the second pass for this reason. All of the results that follow were derived from the second pass dataset.

The largest source of error in the values of IWC_c obtained by this procedure occurred as a result of variations in ρ_e caused by differences in the particle size spectra or particle type within a reflectivity category. This error caused the values of IWC_c to vary by a factor of ~2 in Norbert and by ~3 in Irene. The error in Z_c results from the fluctuations in ρ_e and to a much smaller extent, from variations in the number of the largest particles accepted. These errors caused Z_c to vary by ~5 dBZ in Norbert and ~9 dBZ in Irene.

An alternate procedure that directly estimates ice water content from Z_m is the method of Plank et al. (1980). As presented by Heymsfield and Palmer (1986) (method 1 in their paper), this procedure consists of deriving a factor K from the reflectivity and ice water content computed from each particle-size spectrum:

$$K = \mathrm{IWC}_c / Z_c{}^{0.5}. \quad (5)$$

The K are used to compute ice water contents at the aircraft from the observed flight-level radar reflectivity estimates:

$$\mathrm{IWC}_r = K Z_m{}^{0.5}, \quad (6)$$

where IWC_r is the ice water content estimate, K is from the particle-size spectrum closest in time to Z_m, and Z_m is the observed radar reflectivity estimate. The val-

ues of IWC_r and Z_m obtained by this method can also be used to derive Z–IWC relations. Heymsfield and Palmer (1986) showed that in the absence of strong gradients of either radar reflectivity or particle number concentration, IWC_r is less sensitive than IWC_c to errors in particle size and mass. That condition is not often satisfied near the hurricane eyewall or the rainbands.

With each of these methods, the reflectivity and ice water content were required to be ≥ 1 dBZ and ≥ 0.02 g m^{-3}. Differences in the number of spectra used to construct the fit lines for the two-pass method and the Plank method arise because of the differences between Z_c, Z_m, IWC_c, and IWC_m.

3. Results

A scatter plot of the $\log_{10}(IWC_c)$ and the dBZ_c from the Norbert stratiform data is shown in Fig. 1. All of the calculated reflectivities were in the range $1 \leq dBZ \leq 34.5$, and the measured reflectivity varied from $1 \leq dBZ \leq 34$. Calculated ice water contents were in the range $0.02 \leq IWC_c \leq 1.9$ g m^{-3}. The stratiform dataset contained 874 particle-size spectra. Most of the particles were irregular snow and columns.

Table 2 shows ρ_e as a function of Z_m and the percentage of the 10 s average particle-size spectra that were used to compute it. Reflectivity categories that contain $> \sim 10\%$ of the sample are reasonably well sampled; such categories include >80 particle-size spectra. All reflectivities ≤ 25 dBZ are well represented in the stratiform data. The mean value of ρ_e varied little with reflectivity through 25 dBZ and was ~ 0.05 g cm^{-3}. These values were computed from all particle-size spectra within a given reflectivity category from each storm and are similar to the 0.09 g cm^{-3} value for ρ_e that was derived by Passarelli et al. (1976) from radar and OAP-1DP probe (a simpler version of the 2D-P) data collected in a snowstorm over central Illinois. Differences in ρ_e within a particular reflectivity category between data files arise because of differences in the mix of ice particle types, sizes and concentration at different places and times that have similar reflectivity. These variations show that it is necessary to compute ρ_e frequently within a dataset to obtain the most accurate estimate of IWC possible.

Hurricane Irene (1981) provided 870 data points (Fig. 2). Almost all of these samples were obtained inside and near a vigorous convective band (Black and Hallett, 1986). Many of these samples had $Z_c > 30$ dBZ, and some were >40 dBZ. Only the range $15 < dBZ_m \leq 35$ is well represented, but this range spans most of the reflectivities encountered in the near glaciated hurricane convection. These data were much more scattered than the stratiform data and the values of ρ_e were also higher. Effective ice particle bulk densities were calculated for the Irene data in the same way as for Norbert. The mean ρ_e for the Irene convective data increased with reflectivity from 0.08–0.69 g m^{-3}.

4. Discussion

Table 3 presents the Z–IWC relations that were derived for hurricane stratiform and convective areas, respectively, and a composite relation computed from all of the hurricane data. Both results from the two-pass method and the approach of Plank et al. (1980) are given. Both the exponents and coefficients of the equations produced by the Plank et al. (1980) method were smaller than those of the two-pass method. This result occurs because the tail radar's sample volume is much larger than that of the 2D-P, so horizontal re-

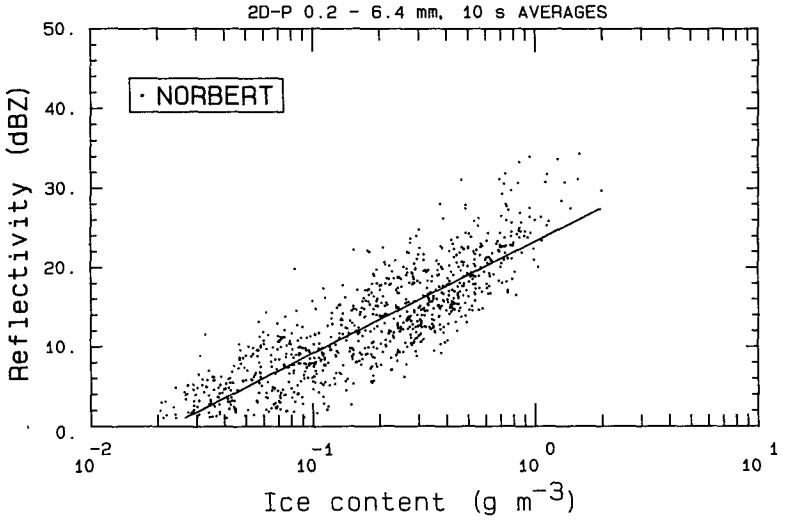

FIG. 1. Scatter plot of the IWC–dBZ data from Hurricane Norbert. The least-squares fit line is shown.

TABLE 2. Reflectivity–effective ice particle bulk density for hurricanes. Category size is the percentage of size distributions in each reflectivity range. There were 874 size distributions in the Norbert (stratiform) sample, and 870 in the Irene (convective) sample.

Measured reflectivity (dBZ)	Mean ρ_e (all data) (g cm^{-3})	Density range (between files)	Category size (%)
	Hurricane Norbert		
>0–≤05	0.03	0.01–0.06	9.6
>05–≤10	0.05	0.02–0.06	21.9
>10–≤15	0.05	0.03–0.08	26.1
>15–≤20	0.05	0.04–0.07	21.4
>20–≤25	0.10	0.04–0.26	12.9
>25–≤30	0.24	0.11–0.31	3.2
>30–<35	0.37	0.26–0.39	0.7
	Hurricane Irene		
>0–≤05	0.08	0.03–0.10	1.3
>05–≤10	0.23	0.03–0.40	4.0
>10–≤15	0.20	0.09–0.61	7.1
>15–≤20	0.26	0.06–0.43	15.4
>20–≤25	0.16	0.08–0.56	34.3
>25–≤30	0.28	0.10–0.61	20.8
>30–≤35	0.59	0.40–0.74	9.7
>35–≤40	0.69	0.62–0.73	7.5

flectivity gradients tend to be largest in Z_c. Thus, the Plank et al. (1980) method works to raise the IWC at low reflectivity and lower IWC at high reflectivity in comparison with the two-pass method. This effect is also present in Table 2 of Heymsfield and Palmer (1986). The composite equations given in Table 3 were computed for all available spectra with $Z_c \geq 1$ dBZ and IWC$_c \geq 0.05$ g m^{-3}. These limits were chosen to produce a composite that better represents the bulk of the spectra.

TABLE 3. Least-squares fit lines for the indicated data. The units of IWC are g m^{-3}.

	N	r^2	Notes[a]
$Z = 219*(\text{IWC})^{1.40}$	874	0.72	HS
$Z = 915*(\text{IWC})^{1.51}$	870	0.65	HC
$Z = 670*(\text{IWC})^{1.79}$	1609	0.65	HA
	(Plank et al. 1980 method)		
$Z = 192*(\text{IWC})^{1.22}$	902	0.74	HS
$Z = 875*(\text{IWC})^{1.24}$	865	0.63	HC
$Z = 575*(\text{IWC})^{1.58}$	1667	0.65	HA

[a] HS: Norbert (stratiform) dataset. HC: Irene (convective) data. HA: Composite of all hurricane data.

The comparison of the hurricane dBZ–log$_{10}$ (IWC) regression lines in this study with the midlatitude lines that were derived by other researchers is shown in Fig. 3. A small slope in the dBZ–log$_{10}$ (IWC) relation indicates that proportionally more water is concentrated in the smallest particles. Similarly, the intercept is directly proportional to the IWC. In the context of the water budget, an increase in the slope of the regression line would allocate a higher proportion of the total water to the precipitation water content. Likewise, an increase in the intercept of the dBZ–log$_{10}$ (IWC) relation for a fixed slope would indicate a higher total amount of water.

The 15–45 dBZ range of the hurricane convection line resembles the Herzegh and Hobbs (1980) line, which was computed from data collected in warm frontal convective and stratiform clouds. Also, the hurricane stratiform line is almost identical to the Heymsfield and Palmer (1986) thunderstorm anvil line. In both cases, the hurricane lines have slightly

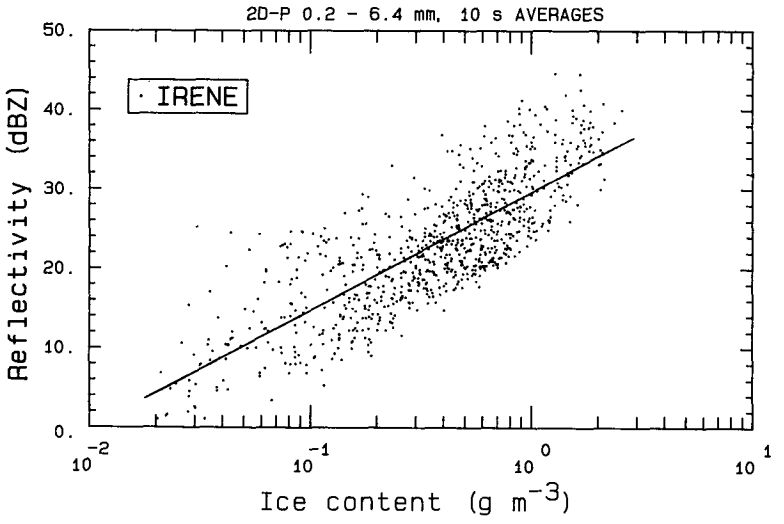

FIG. 2. As in Fig. 1, but for Hurricane Irene.

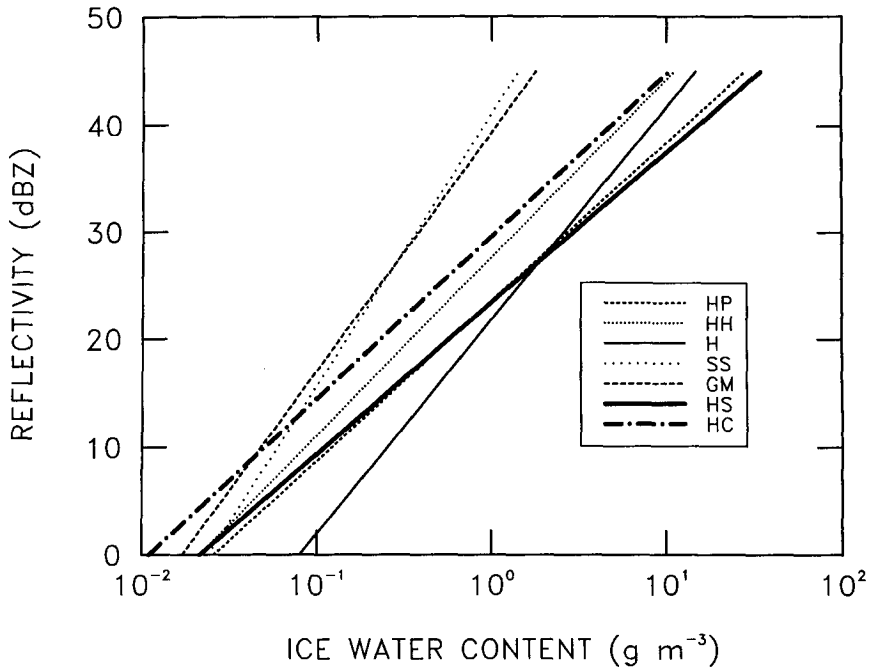

FIG. 3. Comparison of earlier Z–IWC relations with those from hurricanes. Abbreviations for the other lines are the same as the Tables 1 and 2.

smaller slopes and approximately equal intercepts in comparison to the midlatitude lines. The steepness of the fit lines from Gunn and Marshall (1958), Sekhon and Srivastava (1970), and to a lesser extent Heymsfield (1977) with respect to the hurricane fits indicate that their data lacked smaller ice particles. Small ice particles would increase the IWC without greatly increasing the reflectivity.

5. Conclusions

Airborne radar reflectivity data (Z) and ice water content (IWC) derived from particle image data were obtained in the convective regions of Hurricane Irene and the stratiform areas of Hurricane Norbert. Regression equations relating Z and IWC are presented for a two-pass method and the procedure described by Plank et al. (1980). Both methods give similar results, although the exponents on the Plank et al. (1980) equations (Table 3) are slightly smaller.

The exponents of the regression equations are nearly equal in the convective and stratiform areas. However, the coefficient for the convective areas is much larger than that for the stratiform regions. The Student's t-test shows that the difference between the coefficients is significant at the 1% level. This difference is a consequence of the larger effective ice particle bulk density of the graupel in Irene relative to that of the snow in Norbert and the greater relative abundance of large-diameter particles in the Irene data. These results suggest that the Z–IWC relations are dissimilar in the convective and stratiform areas of hurricanes.

The hurricane Z–IWC regression equations were compared with a wide range of Z–IWC relations for frontal clouds, snowstorms, and the anvils of midlatitude thunderstorms. The convective Z–IWC relation from Hurricane Irene corresponds reasonably well to the equation determined by Herzegh and Hobbs (1980) for warm frontal clouds, particularly for reflectivities from 15–45 dBZ which represent >90% of the hurricane sample. Since the Herzegh and Hobbs (1980) data set also contained convective clouds, this study suggests that convective clouds need separate Z–IWC relations. The stratiform Z–IWC relation is similar to the equations for the anvil region of Montana thunderstorms derived by Heymsfield and Palmer (1986). The close correspondence of the regression equations for the stratiform areas of hurricanes and midlatitude thunderstorm anvils indicates that the ice water content and structure of glaciated stratiform clouds may be similar regardless of differences in temperatures and latitude. The fits of Gunn and Marshal (1958), Sekhon and Srivastava (1970), and Heymsfield (1977) have much steeper slopes than the other fits. This effect would occur if few small ice particles were present in their data.

Acknowledgments. I would like to thank Drs Robert Burpee, John Gamache, and Andrew Heymsfield for their helpful comments and criticisms. Paul Willis and

Peter Dodge provided helpful internal reviews of the manuscript. Also, thanks are extended to the flight crews of NOAA/AOC, whose hard work made this study possible.

REFERENCES

Battan, L. J., 1973: *Radar Observation of the Atmosphere.* University of Chicago, 324 pp.

Black, R. A., and J. Hallett, 1986: Observations of the distribution of ice in hurricanes. *J. Atmos. Sci.*, **43,** 802–822.

Gunn, K. L. S., and J. S. Marshall, 1958: The distribution with size of aggregate snowflakes. *J. Meteor.*, **15,** 452–461.

Herzegh, P. H., and P. V. Hobbs, 1980: The mesoscale and microscale structure and organization of clouds and precipitation in mid-latitude cyclones. II: Warm-frontal clouds. *J. Atmos. Sci.*, **37,** 597–611.

Heysmefield, A. J., 1977: Precipitation development in stratiform ice clouds: A microphysical and dynamical study. *J. Atmos. Sci.*, **34,** 367–381.

——, and A. G. Palmer, 1986: Relationships for deriving thunderstorm anvil ice mass for CCOPE storm water budget estimates. *J. Climate Appl. Meteor.*, **25,** 691–702.

Jorgensen, D. P., E. J. Zipser and M. A. Lemone, 1985: Vertical motions in intense hurricanes. *J. Atmos. Sci.*, **42,** 839–856.

Knollenberg, R. G., 1981: Techniques for probing cloud microstructure. *Clouds, Their Optical Properties and Effects.* P. V. Hobbs, A. Deepak, Eds., Academic Press, 15–89.

Marks, F. D., Jr., and R. A. Houze, Jr., 1987: Inner core structure of Hurricane Alicia from airborne Doppler radar observations. *J. Atmos. Sci.*, **44,** 1296–1317.

Passarelli, R. E., Jr., N. J. Carrera and R. R. Braham, Jr., 1976: Comparison of radar and aircraft measurements of snow size spectra in a Midwest winter snowstorm. *17th Conf. on Radar Meteorology,* Seattle, Amer. Meteor. Soc., 214–219.

Plank, V. G., R. O. Berthel and A. A. Barnes, 1980: An improved method for obtaining the water content values of ice hydrometeors from aircraft and radar data. *J. Appl. Meteor.*, **19,** 1293–1299.

Sekhon, R. S., and R. C. Srivastava, 1970: Snow size spectra and radar reflectivity. *J. Atmos. Sci.*, **27,** 299–307.

Smith, P. L., 1984: Equivalent radar reflectivity factors for snow and ice particles. *J. Climate Appl. Meteor.*, **23,** 1258–1260.